TURBULENCE CHARACTERISTICS OF COUETTE-POISEUILLE TURBULENT FLOWS

Koichi NAKABAYASHI
Department of Mechanical Engineering, Nagoya Institute of Technology
Gokiso-cho, Showa-ku, Nagoya 466-8555, Japan
nakabaya@cfd.mech.nitech.ac.jp

Osami KITOH
Department of Mechanical Engineering, Nagoya Institute of Technology
Gokiso-cho, Showa-ku, Nagoya 466-8555, Japan
kitoh@cfd.mech.nitech.ac.jp

Yoshitaka KATOU
Toyota Communication System Co., Ltd.
Higashi-Sakura Daiichi Bldg. 7F, Higashi-Sakura, Higashi-ku,
Nagoya 461-0005, Japan
yoshi-kato@toyota-cs.com

ABSTRACT

Turbulence characteristics of Couette-Poiseuille turbulent flow (C-P flow) have been studied experimentally. In the wall region, turbulence characteristics are strongly influenced by dimensionless parameter of the shear stress gradient μ, but not much by Reynolds number Re*. In the core-region, however, there is a great difference in the distribution of turbulence intensity between P- and C-types. For P-type, an effective friction velocity and a new coordinate $\eta=y-\delta_p$ can be used for the universal profile, whereas for C-type, the local scaling and the wall coordinate y are adequate. For $\mu=0\sim55$, the sweep event contributes more to the Reynolds shear stress than that by ejection.

INTRODUCTION

In the study of turbulence structure in C-P flow, the work by El Telbany & Reynolds (1981) may be considered a typical experimental article, although Thurlow & Klewicki (2000) reported an investigation on the so-called "geometry effect" recently. Kuroda et al. (1994), on the other hand, studied the effect of mean shear rate on the wall turbulence by numerical simulation. But no systematic studies on turbulence statistics have been published on C-P flows so far except for that by El Telbany & Reynolds, who studied similarity laws of turbulence intensity in addition to turbulent kinetic energy and correlation coefficient etc. However the inlet length influenced their measurements, so the present investigation has been conducted in the fully developed condition.

The main objective of this work is to clarify the effect of the shear stress gradient on the structure of wall turbulence. A specific character of the C-P flow is that the shear stress distribution is linear. This is the basic reason we have studied this flow. The global parameters of C-P flows are the Reynolds number $Re^*=u_*h/\nu$, dimensionless parameter of shear stress gradient $\mu=u_*^3/(\alpha\nu)$ and flow type parameter $\beta=\alpha h/u_*^2$. Here u_*, h, $\alpha=d(\tau/\rho)/dy$ and y stand for friction velocity based on the shear stress at the stationary wall, the channel half height, the kinematic shear stress gradient and the distance from the stationary wall. The values of these parameters can be changed independently by selecting various combinations of bulk flow-velocity (flow rate) and moving wall speed in the C-P flow. Thus, we can investigate each effect of these parameters separately on the similarity laws of turbulence statistics. However, plane Poiseuille flow, a particular case of C-P flow, has a relation of $Re^*=-\mu$. Accordingly, we can not set different values of Re* and μ in the plane Poiseuille flow. In the present paper, similarity laws of turbulence intensities, correlation coefficient, skewness factor and four-quadrant analysis of Reynolds shear stress are discussed.

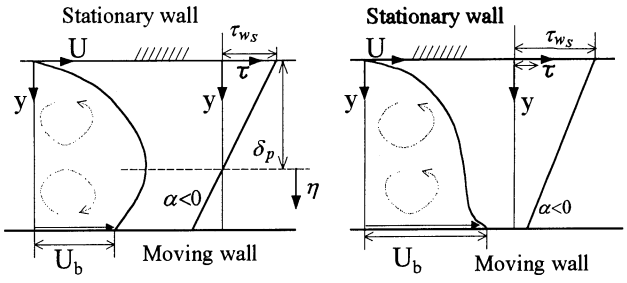

Poiseuille-type flow Couette-type flow

Figure 1 : Mean velocity profile and shear stress distribution of P- and C-type flows.

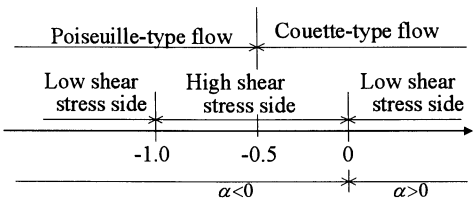

Figure 2 : Relation among α, β and flow type.

FLOW CHARACTERISTICS AND SIMILARITY LAWS

The C-P flow can be distinguished into Poiseuille-type (P-type) and Couette-type (C-type), as shown in figure 1. An upper wall is stationary and a lower wall is moving. The subscripts s and m denote the stationary and moving walls, respectively. In P-type, the position of $\tau=0$, i.e. $y=\delta_p=u_*^2/|\alpha|$ that nearly equals the position of maximum velocity, exists in the flow field between the walls, and the value of α must be negative. For C-type, however, the value of α becomes positive or negative, depending on the speed of the moving wall, on which the maximum velocity exists. And the location of $\tau=0$ does not exist in the flow field. The relation among α, β and flow type is shown in figure 2, where P- or C-type can be realized for $\beta<-0.5$ or >-0.5. In particular, plane Poiseuille and Couette flows can be realized for $\beta=-1$ and 0, respectively.

Since clear conclusions on turbulence intensities have not been obtained, we summarize the relations obtained by dimensional analysis before we consider them on the basis of the present experimental results. In the wall region, the following equation can be written:

$$u'/u_*=u'^+=f_1(y^+,\mu,\mathrm{Re}^*). \quad (1)$$

As described later, Re* is less effective than μ, so u'^+ can also be written by

$$u'^+=f_2(y^+,\mu). \quad (2)$$

As the wall is approached, this equation can be expanded by Taylor series.

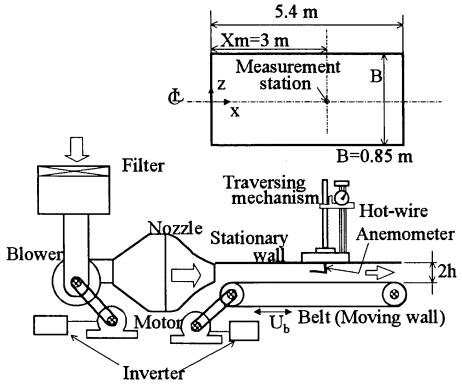

Figure 3 : Experimental apparatus.

$$u'^+=A_1(\mu)y^+ + A_2(\mu)y^{+2} \quad (3)$$

Very close to the wall, the higher order terms are omitted.

$$u'^+=A_1(\mu)y^+ \quad (4)$$

When the values of both y^+ and μ are large, the "plateau" region appears.

$$u'^+=B \quad (5)$$

A turbulent core region exists in the central part of the channel, where different velocity scales and coordinates should be used depending on C- or P-type. For P-type, a new coordinate η defined by $\eta=y-\delta_p$ and an effective friction velocity u_e defined by $u_e=(|\alpha|h)^{1/2}=[(u_{*s}+u_{*m})/2]^{1/2}$ are recommended For C-type, the velocity scale should be based on a local friction velocity $u_L=(\tau/\rho)^{1/2}$. Consequently, the following relations can be obtained:

$$u'/u_e = f_3(\eta/h,\beta) \quad (6)$$

for P-type and

$$u'/u_L = f_4(y/h,\beta) \quad (7)$$

for C-type.

EXPERIMENTAL APPARATUS AND METHOD

Figure 3 shows a schematic view of the test channel, which is 5.4 m in length and 0.85 m in width. An upper wall is stationary and a lower wall which consists of a flat belt can be moved either with the air blown through the channel or in the opposite direction. The channel depth 2h=20, 40 and 80 mm. The belt speed was measured optically by counting the number of tape strips passing through the sensor per second. Two motors to drive the blower and the belt were controlled by inverter units. Pressure holes were equipped on the stationary wall, every 200 mm in the x-direction, and the static pressure was measured at these points by a precision pressure cell.

The measurements of velocity were made at the center of the channel at station $x_m=3$ m from the inlet of the channel, where the flow was fully developed. We measured mean velocity profiles and streamwise and normal fluctuating velocity components (u and v) by hot-wire anemometers with I- and X-type probes, respectively. The reliability of measurements was checked by comparison of Reynolds shear stress between the data measured directly by X-wire and the results calculated from the momentum balance equation using the mean velocity profiles. The result shows that the present data are reliable within an accuracy of less than 1% uncertainty for the mean velocity and about 4% uncertainty for Reynolds stress except for extremely close to the wall. The friction velocity u_* was estimated from the mean

Figures 7 and 8 show distributions of turbulence intensities scaled by u_e and u_L according to equations (6) and (7) in the turbulent core-region for P- and C-types, respectively. For P-type, the results obtained by El Telbany & Reynolds (1981) are higher and more widely scattered than the present results, which are distributed around a line for plane Poiseuille flow. The minimum value at η=0 increases approximately with decreasing β. For C-type, the present results are higher than those of Telbany & Reynolds (1981). Around the central part of the channel, the profile increases with Re* and approaches that of plane Couette flow as β approaches 0.

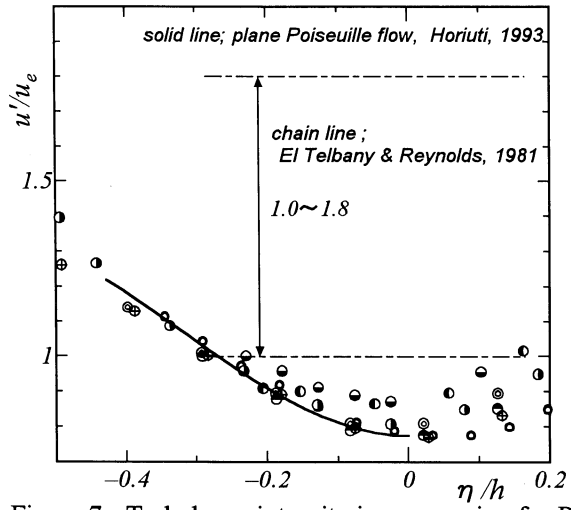

Figure 7 : Turbulence intensity in core-region for P-type.

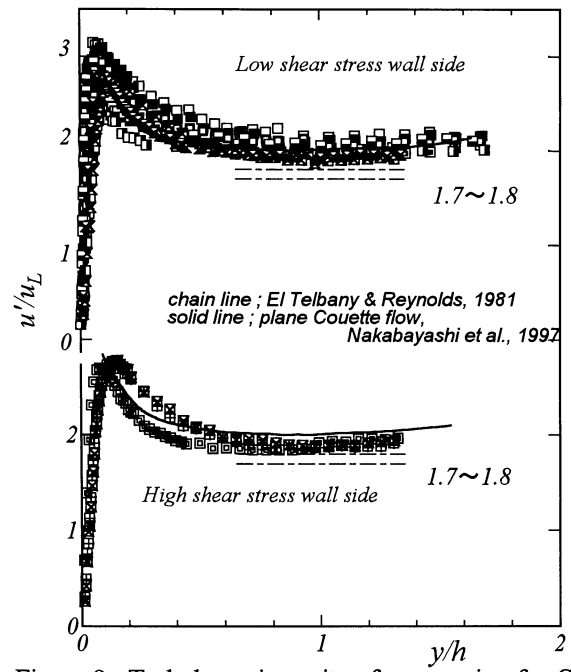

Figure 8 : Turbulence intensity of core-region for C-type.

Shear correlation coefficient

Figure 9 shows variations of the shear correlation coefficient against y/h for C-type. Note that C-type has no zero-correlation point in the channel as P-type does. Except for the near wall region, i.e., y/h>0.4, the correlation coefficient has a value of about 0.45 at its maximum that is typical of turbulent uniform shear flow, Tavoularis & Karnik (1989). El Telbany & Reynolds (1981) reported a much larger value of 0.7~0.75 for C-type as shown by chain line in the figure. The measuring section in their experiment was (45~20)×(2h) from the inlet section, compared with (150~37)×(2h) in our experiment. this was too short to obtain the turbulent statistics of fully developed flows.

Skewness factor

Figure 10 shows distributions of the skewness factor for u-component S(u) against y^+ for various μ and Re*. The solid and dotted lines indicate the experimental results of plane Couette flow (μ=∞, Re*=253, Nakabayashi et al., 1997) and DNS for plane Poiseuille flow (Re*=180, Horiuti, 1993), respectively.

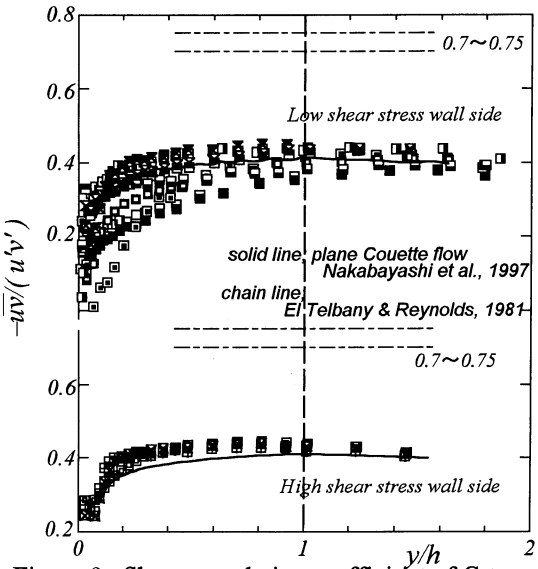

Figure 9 : Shear correlation coefficient of C-type.

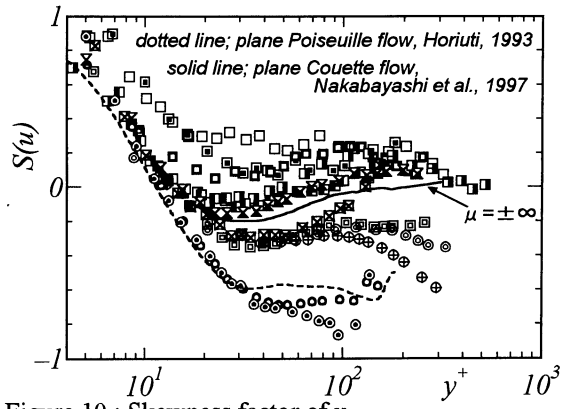

Figure 10 : Skewness factor of u.

velocity profiles near the wall, based on the principle proposed by Bahtia et al. (1982) and the procedure used of Nagano et al. (1991).

EXPERIMENTAL RESULTS AND DISCUSSION

The table shows the symbols used in the figures to follow. The values of parameters in the table are based on the stationary wall (y=0) side for both P- and C-types.

Turbulence intensities

Figure 4 shows the variations of u^{+} according to the wall-stress scaling of equation (1). From comparing the results with the close value of μ but different Re* with each other, the profiles do not differ so much, i.e., influence of Re* is small, so that equation (2) is adequate and equation (4) holds for $y^{+}<6$. The value of $A_1(\mu)$ increases or decreases with a decrease of $|\mu|$ for $\mu>0$ or $\mu<0$. The value of u^{+} increases or decreases from the values of $\mu=\infty$ for $\mu>0$ or $\mu<0$, as $|\mu|$ decreases.

Poiseuille–type				Couette–type			
	μ	Re*	β		μ	Re*	β
●	−60	100	−1.66	⊠	−1334	105	−0.08
◉	−127	96	−0.76	⊞	−464	112	−0.24
○	−137	164	−1.20	▣	−413	175	−0.42
◑	−195	277	−1.42	■	35	156	4.48
◐	−216	455	−2.11	□	55	177	3.23
◓	−264	370	−1.40	▣	85	103	1.22
◒	−275	653	−2.37	◘	94	145	1.54
◎	−376	568	−1.51	◨	222	278	1.25
⊕	−383	421	−1.10	◧	258	99	0.38
⊗	−531	679	−1.28	▬	451	160	0.35
				▭	780	316	0.41
				⧓	902	100	0.11
				⧗	1333	159	0.12

Table : Parameters and symbols.

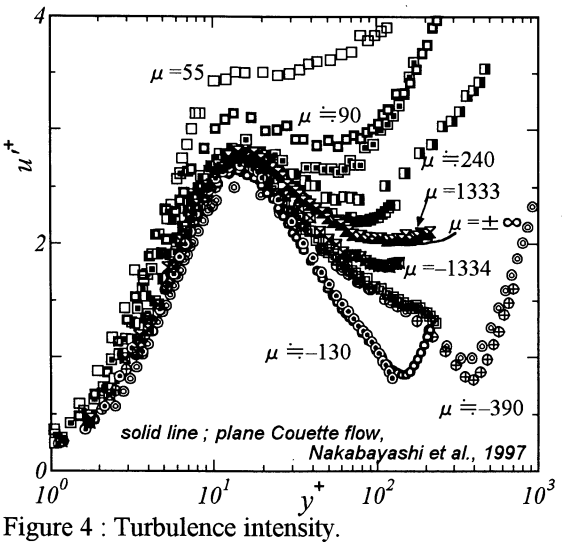

Figure 4 : Turbulence intensity.

This tendency derives from the variation of turbulent kinetic energy production $(-\overline{uv}(dU/dy)(\nu/u_*^4)) = (-\overline{uv}^{+}(dU^{+}/dy^{+}))$ with μ, as shown in figure 5. Here for $\mu>0$, the dimensionless Reynolds shear stress $(-\overline{uv}^{+})$ increases with μ^{-1}, while dU^{+}/dy^{+} does not change much with μ. Thus it assures a large production rate of turbulent kinetic energy for small positive μ. For $\mu<0$, however, the location of $\tau=0$, at which no production of the kinetic energy occurs, approaches the wall with increasing $|\mu|^{-1}$. Hence, as $|\mu|$ decreases, the intensity profile shifts downward, as seen in figure 4. Since the relation $Re^{*}=-\mu$ holds in the plane Poiseuille flow, it is appropriate to understand that the variations of turbulence intensities' so-called "low Reynolds number effect" is caused by the μ effect. When the values of both μ and y^{+} are large, say $\mu=1{,}333$ and $y^{+}=80\sim100$ in figure 4, the "plateau" region appears, where equation (5) holds. Figure 6 shows the peak values of u'^{+}, u'^{+}_{peak}, and its location, $y^{+}_{u'peak}$, against $|\mu|$. There is difference in the relations between C-P flows and the turbulent boundary layers. This suggests the existence of some differences in the turbulence structure for $y^{+}>15$.

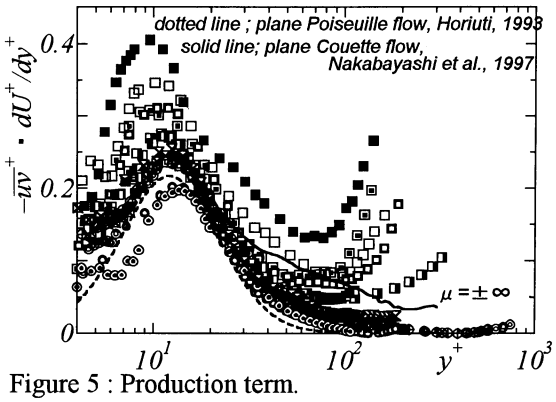

Figure 5 : Production term.

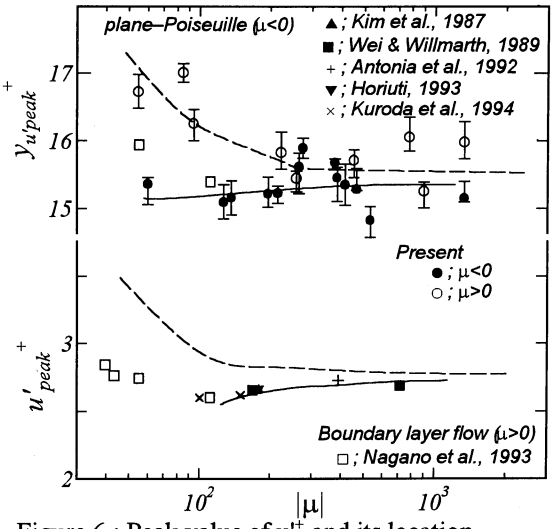

Figure 6 : Peak value of u'^{+} and its location.

In the wall region variations of S(u) having nearly the same μ but different Re* are almost the same. This indicates that Re* does not have an appreciable effect on the S(u) profile as μ does. Such a Re*-independence is similar to the turbulence intensity profiles as described in the Subsection on "Turbulence intensities". In general, S(u) increases (when $\mu>0$) or decreases (when $\mu<0$) from the value of $\mu=\infty$ (plane Couette flow) as $|\mu|$ decreases. For $\mu>0$, the upward deviation of each profile from that of $\mu=\infty$ is more significant as the wall is approached. This can be explained as follows. As shown in figure 4, the turbulent motion becomes more and more active in the region away from the wall as μ (>0) decreases and the high velocity there penetrates inside the near wall region which causes the strong sweep event. This is the reason for the noticeable increase of S(u) near the wall for $\mu>0$. In particular, as μ decreases below 94, negative S(u) disappear from the channel section because the intensified sweep contributes to the Reynolds shear stress more than the ejection as shown in the next section. For $\mu<0$, however, S(u) shifts downward from $\mu=\infty$ in the region away from the wall.

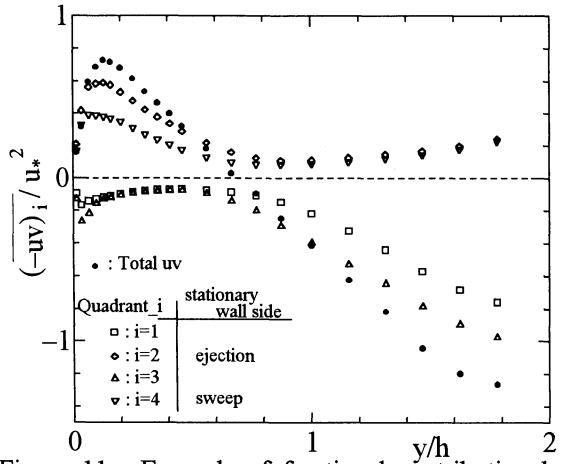

Figure 11 : Example of fractional contribution by four-quadrant analysis. P-type (Re*=277, μ=-195).

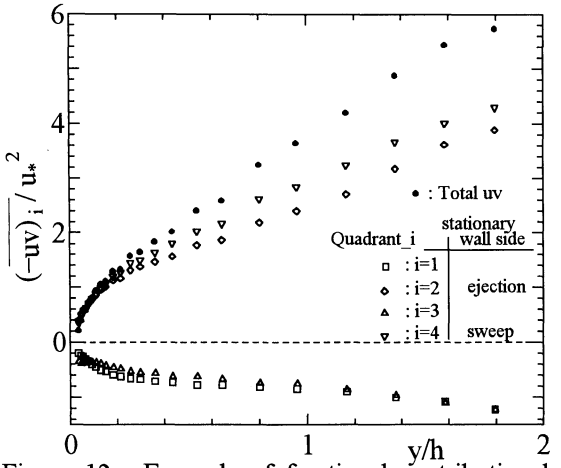

Figure 12 : Example of fractional contribution by four-quadrant analysis. C-type (Re*=156, μ=35).

This can be explained as follows. In the case of $\mu<0$, the turbulence intensity and/or the turbulent kinetic energy production in the outer wall region become more and more weak compared with that in the buffer region as $|\mu|$ decreases. And the ejection of low speed velocity into the outer wall region overwhelms the sweep as described in the next section. In the region of y^+ less than about 10, however, negative μ has no effect on S(u) at all, so the ejection and the sweep events are presumably unaltered.

Four-quadrant analysis of fluctuating velocities

Frequencies and fractional contributions to the Reynolds shear stress from each velocity quadrant are studied by four-quadrant analysis. Figure 11 gives typical example of P-type (μ=-195, Re*=277). Here $-(\overline{uv})_i$ stands for the contribution to the Reynolds shear stress from i-quadrant. The figures give the correspondences between the type of events (ejection, sweep and interaction) and each quadrant. Variations of fractional contribution and frequency against y/h for P-type are similar with those of plane Poiseuille flow, i.e., contribution from the ejection with small frequency is larger than from the sweep in either wall sides. Figure 12 shows an example of the fractional contribution of C-type with a large positive shear stress gradient (μ=35, Re*=156). Contrary to P-type, the sweep contributes more to the Reynolds shear stress than ejection.

The effect of μ on the fractional contribution is different between P- and C-types. To see the effect, the relative fractional contributions defined as $-(\overline{uv})_i/(-\overline{uv})$, i=2 and 4, are plotted against y^+ for various μ in figures 13 and 14 for C-type, respectively. The relative fractional contribution from quadrant-2 is not affected much by μ. The value for i=4, however, increases near the wall (y^+<100~200) as positive μ decreases.

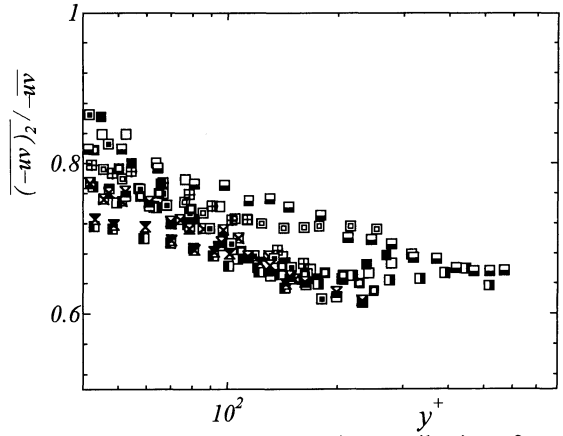

Figure 13: Relative fractional contribution from quadrant_2 for C-type.

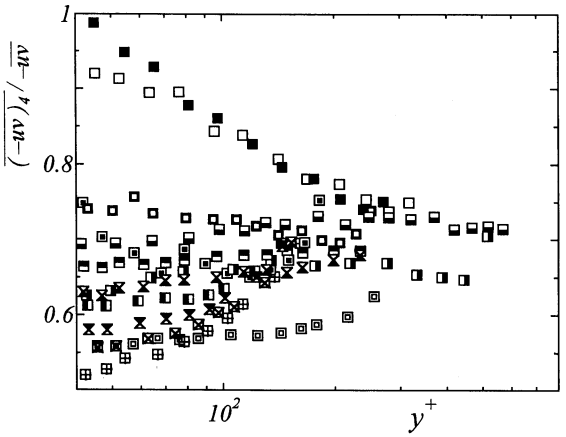

Figure 14 : Relative fractional contribution from quadrant_4 for C-type.

Thus the contribution from sweep becomes stronger as μ decreases and, finally when μ decreases below around 50, sweep prevails over ejection. This is a particular feature of C-type turbulence with a large positive shear stress gradient. For P-type (not shown), the value for ejection near the wall is 0.75~0.85, showing no appreciable change with μ whereas for sweep it is below 0.6 and decreases with decreasing $|\mu|$. Thus in the range of $40 \leq y^+ \leq 80$ the contribution from ejection becomes more and more dominant than sweep as $|\mu|$ decreases.

CONCLUSIONS

The main conclusions obtained are as follows.

(1) Similarity laws for the turbulence intensity variation can be expressed as functions of Re* and shear stress gradient parameter μ (or β), by equations (2), (4), (5), (6) and (7). Similar laws hold for the skewness factor. The experimental results confirm these similarity laws. In the wall region, μ is a governing parameter whereas Re* has little effect on the similarity law.

(2) Because the relation $Re^*=-\mu$ holds in plane Poiseuille flow and Re* has little effect on the similarity laws for C-P flows, the low Reynolds number effect for plane Poiseuille flow on turbulence quantities can be attributed to μ effect.

(3) The turbulence activity away from the wall is extremely high for $\mu>0$ or low for $\mu<0$. Thus a strong sweep plays a dominant role in Reynolds shear stress when $0<\mu<50$, whereas strong ejection from the near wall region prevails in the case of negative μ having small absolute value.

This work was supported through the Grant-in-Aid (No. 03452123) in 1991-1995 by the Japan Ministry of Education, Science and Culture.

REFERENCES

El Telbany, M.M.M. and Reynolds, A. J., 1981, "Turbulence in Plane Channel Flows", J. Fluid Mech., vol. 111, pp. 283-318.

Thurlow, E.M. and Klewicki, J.C., 2000, "Experimental study of turbulent Poiseuille-Couette flow", Physics of Fluids, vol. 12, pp. 865-875.

Kuroda, A., Kasagi, N. and Hirata, M., 1994, "Direct numerical simulation of turbulent Couette-Poiseuille flows: Effect of mean shear rate on the near-wall turbulent structures", Turbulent Shear Flows, vol. 9, Ed. by Durst et al., Springer, pp.241-257.

Bahtia, J.C., Durst, F. and Jovanovic, J., 1982, "Correlation of Hot-Wire Anemometer Measurements Near Walls", J. Fluid Mech., vol. 122, pp. 411-431.

Nagano, Y., Tagawa, M. and Tsuji, T., 1993, "Effects of Adverse Pressure Gradients on Mean Flows and Turbulence Statistics in a Boundary Layer", Turbulent Shear Flows, vol. 8, Ed. by Durst et al., Springer, pp. 7-21.

Nakabayashi, K., Kitoh, O. and Nishimura, F., 1997, "Experimental Study of a Turbulent Couette Flow at Low Reynolds Number", Proc. 11th Symp. Turbulent Shear Flows, pp. 11-10—11-15.

Wei, T. and Willmarth, W.W., 1989, "Reynolds Number Effects on the Structure of Turbulent Channel Flow", J. Fluid Mech., vol. 204, pp.57-95.

Antonia, R.A. Teitel, M., Kim, J. and Brown, L.W.B., 1992, "Low-Reynolds-Number Effects in a Fully Developed Turbulent Channel Flow", J. Fluid Mech., vol. 236, pp. 579-605.

Horiuti K., 1993, "Establishment of the Direct Numerical Simulation Data Bases of Turbulent Transport Phenomena, Co-operative Research No. 02302043 Supported by the Ministry of Education, Science and Culture, 1990-1992".

Kim, J., Moin, P. and Moser, R., 1987, "Turbulence Statistics in Fully Developed Channel Flow at Low Reynolds Number", J. Fluid Mech., vol. 177, pp.133-166.

Tavoularis, S. and Karnik, K., 1989, "Further experiments on the evolution of turbulent stresses and scales in uniformly sheared turbulence", J. Fluid Mech., vol. 204, pp. 457-478.